This article has been accepted for publication in a future issue of this journal, but has not been fully edited. Content may change prior to final publication. Citation information: DOI 10.1109/JLT.2015.2471853, Journal of Lightwave Technology

High Performance Optical Modulator Based on Electro-optic Polymer Filled Silicon Slot Photonic Crystal Waveguide

Xingyu Zhang, Chi-jui Chung, Amir Hosseini, Harish Subbaraman, Jingdong Luo, Alex K-Y. Jen, Robert L. Nelson, Charles Y-C. Lee, and Ray T. Chen

(Invited Paper)

***Abstract*— Silicon-organic hybrid integrated devices have emerging applications ranging from high-speed optical interconnects to photonic electromagnetic-field sensors. Silicon slot photonic crystal waveguides (PCWs) filled with electro-optic (EO) polymers combine the slow-light effect in PCWs with the high polarizability of EO polymers, which promises the realization of high-performance optical modulators. In this paper, a high-speed, power-efficient, low-dispersion, and compact optical modulator based on an EO polymer filled silicon slot PCW is presented. Lattice-shifted PCWs are utilized to engineer the photonic band diagram and thus enable an 8nm-wide low-dispersion spectrum range, which is over an order of magnitude wider than that in modulators based on non-band-engineered PCWs and ring-resonators. A small voltage-length product of $V_\pi \times L$=0.282V×mm measured at 100KHz is achieved by slow-light enhancement, corresponding to an unprecedented record-high effective in-device EO coefficient (r_{33}) of 1230pm/V among silicon-organic hybrid modulators. Excluding the slow-light effect, the actual in-device r_{33} is estimated to be 98pm/V. By engineering the RC time constant via silicon doping and also utilizing a backside gate technique, the 3-dB modulation bandwidth of the device is measured to be 15GHz. In addition, the RF power consumption of the modulator is estimated to be 24mW at 10GHz, and the estimated energy consumption for potential digital modulations is approximately 94.4fJ/bit at 10Gbit/s.**

***Index Terms*—electrooptic modulators, integrated optics, optical interconnects, photonic crystals, polymers, silicon photonics, slow light**

I. Introduction

The combination of silicon photonics and electro-optic (EO) polymers has enabled compact and high-performance hybrid integrated microwave photonic devices [1-3], such as optical interconnects [4, 5], electro-optic modulators [6, 7], and photonic electric-field sensors [8]. The large EO coefficient (r_{33}), ultrafast response time (~1fs), very low dispersion, and spin-coating feature of EO polymers promise low-power consumption, ultra-high speed operation, and ease of fabrication [9-12]. These features are crucial of optical interconnects. Silicon photonics offers the potential of complementary metal–oxide–semiconductor (CMOS) compatible photonic integrated circuits [13, 14]. Silicon photonic crystal waveguides (PCWs) [15, 16] exhibit slow-light effects, which can be used for device miniaturization [17, 18]. Especially, EO polymer filled silicon slotted PCWs [6, 7, 19, 20] further reduce the device size and enhance the device performance by combining the best of these two platforms.

Our group previously demonstrated an EO polymer filled slot PCW modulator with a slow-light-enhanced effective in-device r_{33} of 735pm/V [20], but the device is dispersive at the band edge which limits its operational spectrum range. To address this problem, a band-engineered slot PCW modulator was designed using lattice-shifted PCWs, and an effective in-device r_{33} of 1190pm/V over optical spectrum of 8nm was achieved [21]. Since both of these two generations of devices were demonstrated at kHz or MHz frequency range, the modulation speed of this type of devices still needs to be improved. A new generation of modulators working at GHz frequency regime, also with high modulation efficiency, low energy consumption and large spectrum range, is highly desired for many applications ranging from digital data communications to analog photonic links. In this work, we aim to achieve a high-speed operation of the same device in [21], by doping the silicon PCWs in two levels and thus reducing the RC time constant. In this the following sections, we report the design, fabrication, and characterization results of a high-speed silicon-organic hybrid (SOH) PCW modulator with high modulation efficiency, low power consumption, and low optical dispersion. Due to combined enhancements provided by the slow-light effect in the PCW and the high r_{33} of the EO polymer, the measured voltage-length product ($V_\pi \times L$) of the modulator is 0.282V×mm at 100KHz, and this corresponds to a record-high effective in-device r_{33} of 1230pm/V ever demonstrated. Assisted by a backside gate technique [22, 23], the modulator is demonstrated with a 3-dB bandwidth of 15GHz. Benefiting from the band-engineered PCW, the

Manuscript received xx, xxxx. This work was supported by the Air Force Research Labs (AFRL) under contract # FA8650-12-M-5131.

X. Zhang, C-J. Chung and R. T. Chen are with the Microelectronic Research Center, Department of Electrical and Computer Engineering, University of Texas, Austin, TX 78758, USA (e-mail: xzhang@utexas.edu; raychen@uts.cc.utexas.edu).

A. Hosseini and H. Subbaraman are with Omega Optics, Inc., 8500 Shoal Creek Blvd, Austin, TX 78757, USA.

J. Luo and A. K-Y. Jen are with Department of Material Science and Engineering, University of Washington, Seattle, WA 98195, USA.

R. L. Nelson and C. Y-C. Lee are with Air Force Research Laboratory at Wright Patterson, Dayton, Ohio 45433, USA.

This article has been accepted for publication in a future issue of this journal, but has not been fully edited. Content may change prior to final publication. Citation information: DOI 10.1109/JLT.2015.2471853, Journal of Lightwave Technology

modulation response is demonstrated to be dispersion-less over an optical spectrum range as wide as 8nm, which is a factor of ~10X better than other modulators based on non-band-engineered PCWs [7, 24] and ring resonators [25].

II. Design

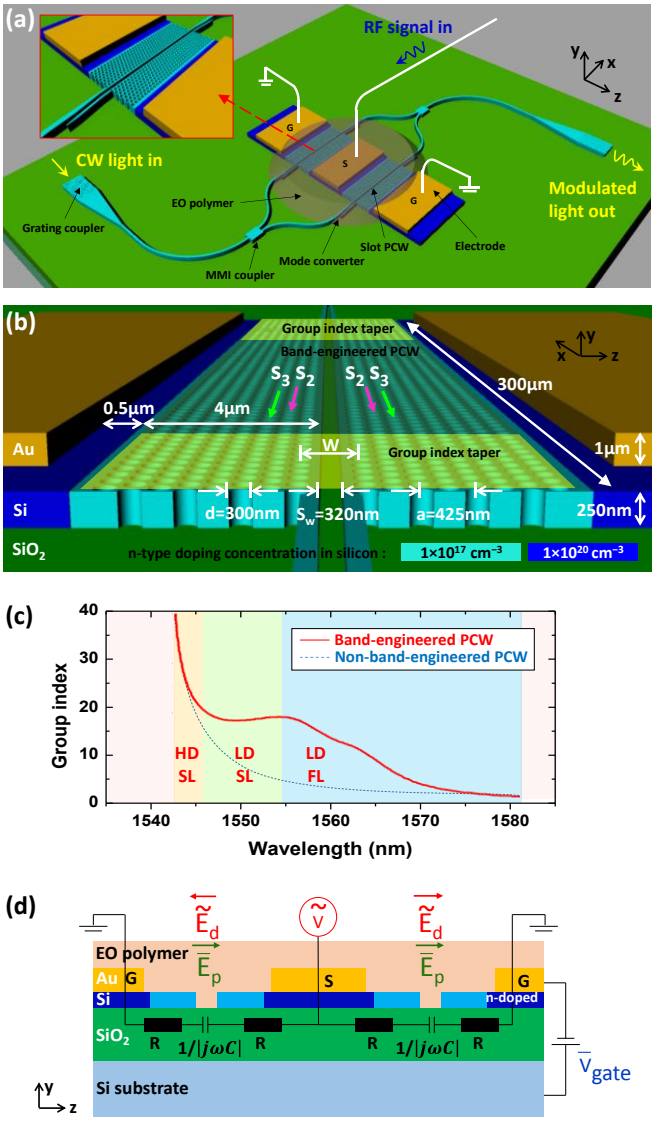

Fig. 1. An EO polymer filled silicon slot PCW MZI modulator designed on an SOI substrate. (a) Three-dimensional schematic of the modulator. The inset shows the magnified image of the silicon slot PCW on one arm of the MZI. PCW: photonic crystal waveguide; MMI: Multi-mode interference; G: ground electrode; S: signal electrode. (b) A tilted view of the slot PCW on one arm of the MZI, showing the cross-sectional device dimension, 2-level doping concentrations, group index taper region, and band-engineered PCW region. Note: the EO polymer is not shown here for better visualization. (c) Simulation result of engineered group index in the slot PCW (red curve) as a function of wavelength for TE mode, showing 8nm low-dispersion slow-light wavelength region (flat band nature of low-dispersion region highlighted in green). Also overlaid is a blue dashed curve representing the dispersive group index versus wavelength for non-band-engineered PCW for comparison. HD SL: high-dispersion slow-light; LD SL: low-dispersion slow-light; LD FL: low-dispersion fast-light. (d) Equivalent electrical circuit of the MZI modulator in a push-pull configuration, with a constant gate voltage applied on the bottom silicon substrate. Ed: driving field, Ep: poling field, Vgate: gate voltage.

Our optical modulator is a symmetric Mach-Zehnder Interferometer (MZI), with slot photonic crystal waveguides (PCWs) incorporated in both the arms, as shown in Fig. 1 (a). We start with a silicon-on-insulator (SOI) substrate with 250nm-thick top silicon and 3μm-thick buried oxide (BOX) layers. The slot and holes of the PCWs are filled with an EO polymer (SEO125 from Soluxra, LLC) which has a refractive index, n=1.63 at 1550nm, and an extraordinary combination of large EO coefficient (r_{33} of ~100pm/V at 1550nm), low optical loss, synthetic scalability and good photochemical stability. Its relatively high glass transition temperature of 150°C provides good temporal stability, and the EO coefficient of poled SEO125 is essentially unchanged under ambient conditions. The refractive index of the EO polymer can be changed by applying an electric field via the Pockels effect, and is given as $\Delta n = -\frac{1}{2} r_{33} n^3 V / S_w$, where Δn is the change in refractive index of the EO polymer, V is the applied voltage, S_w is the slot width. The maximum refractive index change is induced through the EO effect by r_{33} for a lightwave polarized with the z-axis and propagating along x-axis in Fig. 1 (a) when an electric field along the same z-axis is applied; therefore, the PCW is designed for TE polarized light [polarization along z-axis in Fig. 1 (a)]. The slot PCW has a hexagonal lattice of holes with the lattice constant a=425nm, hole diameter d=300nm, slot width S_w=320nm, and center-to-center distance between two rows adjacent to the slot W=1.54($\sqrt{3}$)a. The optimum slot width of 320nm supports a confined optical mode, and also tremendously increases the EO polymer poling efficiency by suppressing the leakage current through the silicon/polymer interface during the poling process [26]. We also note that the poling-induced optical loss is reduced by this reduction of leakage current [27]. More importantly, different from typical slot widths of 100~120nm in conventional slot waveguides [28, 19], widening the slot width to 320nm reduces the slot capacitance, enabling the potential of higher RF bandwidth and lower power consumption, and also relaxes the fabrication complexities. To address the issue of the narrow operational optical bandwidth of typical PCW modulators (less than 1nm at the group index, n_g>10) [7, 24], lattices of the second and third rows of the PCW are shifted parallel to the slot with relative values of S_2 = -85nm, S_3 = 85nm [indicated by the arrows in Fig. 1 (b)]. As a result, a flat group index (n_g) of 20.4 (variations < ±10%) for TE mode over a wavelength range from 1546nm to 1554nm is achieved from simulation, as shown in Fig. 1 (c), enabling an optical spectrum range as wide as 8nm for low-dispersion operation. In order to efficiently couple light from a strip waveguide into and out of the slot PCW, an adiabatic strip-to-slot mode converter is designed [29-31]. To make a smooth transition between the group indices from a slot waveguide (n_g~3) to a slot PCW (n_g~20.4), a group index taper consisting of 8 periods of non-lattice-shifted PCW is developed, in which W increases parabolically from W=1.45($\sqrt{3}$)a to W=1.54($\sqrt{3}$)a [32]. Sub-wavelength gratings (SWGs) are used to couple light into and out of the silicon strips [33]. Multi-mode interference (MMI) couplers are used for beam splitting/combining. The PCW interaction length, L, is chosen to be 300μm for V_π<1V

This article has been accepted for publication in a future issue of this journal, but has not been fully edited. Content may change prior to final publication. Citation information: DOI 10.1109/JLT.2015.2471853, Journal of Lightwave Technology

based on theoretical calculation using $L = \frac{1}{2\sigma} \cdot \frac{n}{\Delta n} \cdot \frac{\lambda}{n_g}$ [34], where σ=0.33 is the overlap integral factor of optical power confined in slot (confinement factor) [35, 36] calculated by the simulation, λ=1550nm is wavelength, and n_g=20.4.

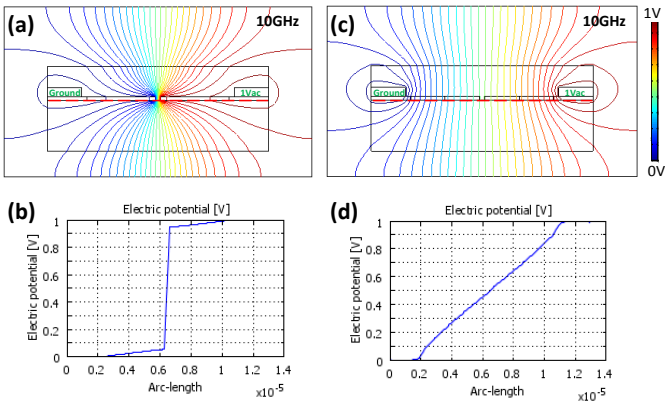

Fig. 2. (a) Simulated electric potential distribution at 10GHz at the cross section of an EO polymer filled doped silicon slot PCW. (b) The voltage drop along the red dashed line in (a). (c) Simulated electric potential distribution at 10GHz across the device without silicon doping as a comparison. (d) The voltage drop along the red dashed line in (c).

Due to the short interaction length (300μm), the maximum modulation frequency of our modulator is not limited by the group velocity mismatch between RF and optical waves, which is usually the case in conventional modulation devices, necessitating the use of complex traveling wave electrode geometries. Instead, it is mainly limited by the time needed to charge the capacitor formed by the slot through the finite ohmic resistance across the silicon; therefore, our modulator can be driven by lumped electrodes, and the RC time delay is the key factor to be engineered for high-speed modulation [6, 37, 3]. The silicon PCW is selectively implanted by n-type dopant (Phosphorus ion, 31P+) with two ion concentrations of 1×10^{20}cm^{-3} and 1×10^{17}cm^{-3} [8], as shown in Figs. 1 (a) and (b), so that the resistivity of silicon region is reduced to 9×10^{-6}Ω·m and 9×10^{-4}Ω·m, respectively [38]. The purpose of using relatively lower concentration (1×10^{17}cm^{-3}) in the waveguide region is to avoid significant impurity-induced optical scattering loss [39, 40]. For reference, the intrinsic doping concentration of the undoped top silicon layer on our SOI wafer is 1×10^{14}cm^{-3}, corresponding to a resistivity of 0.5Ω·m. Based on our previous work [20], in the case of 320nm-wide slots, we use the EO polymer resistivity (ρ_{EO}) value of about 10^8Ω·m and RF dielectric constant ($\varepsilon_{RF,EO}$) value of 3.2. The change in the RF dielectric constant of silicon ($\varepsilon_{RF,Si}$) due to the doping is also taken into account [41].The separation between the gold electrodes is 9.32μm. Figure 1 (d) shows a simplified equivalent circuit of the modulator driven in a push-pull configuration, in which the slot can be represented by a capacitor C and the silicon PCW region by a resistor, R. Effective Medium Approximations [42, 43, 8] are used for the calculation of the effective resistance (R) and the effective RF dielectric constant in the region of EO polymer refilled silicon PCW. As the modulation frequency increases, the percentage of electric potential dropped across the slot will decrease due to the reduced slot impedance (1/|jωC|). The low resistivity of doped silicon can help increase the electric field inside the slot at high frequencies. Figure 2 (a) shows the electric potential distribution at the cross section of the EO polymer filled silicon slot PCW in one arm of the MZI under an AC voltage of 1V at 10GHz, which is simulated by COMSOL Multiphysics. Figure 2 (b) shows the voltage drop along the red dashed line in Fig. 2 (a), in which it can be seen that over 90% of the voltage is dropped across the slot at the RF frequency of 10GHz. Both the optical field and the modulation RF field are concentrated in the 320nm-wide slot, enabling a large field interaction factor, and thus providing efficient modulation at high modulation frequency. As a comparison, Figs. 2 (c) and (d) show the case without silicon doping, in which only 4% of the voltage is dropped across the slot at 10GHz. Based on simulations performed using Lumerical Device software, the total effective resistance of the 300μm-long silicon PCW is 189 Ohms, and the slot capacitance is as small as 39fF. Thus, the theoretical 3-dB modulation bandwidth of the MZI modulator is estimated to be 1/(2πRC)=22GHz. In comparison, the simulation results show that the undoped device has a 3-dB modulation bandwidth below 50MHz.

It was recently demonstrated that the RF bandwidth of modulators can be further improved by applying a constant gate voltage (V_{gate}) between the bottom silicon substrate and top silicon layer [22, 23] to make the top silicon layer sufficiently conductive. This technique avoids the need for heavy doping, so impurity-scattering optical loss can be minimized [44]. This method was used for conventional silicon slot waveguides to achieve modulation up to 42.7GHz [22] and low energy consumption of 320fJ/bit [23]. Here we adopt a similar technique on our silicon PCW modulator, as shown in Fig. 1 (d). By applying a positive voltage on the backside silicon substrate (weakly doped, resistivity of ~0.15Ω·m) across the 3μm-thick BOX layer of our device, the energy bands in the n-type top silicon are bent, and thus more electrons accumulate at the interface between the silicon PCW and the BOX layer. Since the resistivity of the silicon region is inversely proportional to the density and mobility of majority free carriers, the resistivity of the silicon PCW region can be reduced, leading to an enhanced RF bandwidth and a reduced power consumption.

III. Fabrication

The fabrication procedure starts with an SOI wafer. The silicon slot PCW MZI is patterned by electron-beam lithography and reactive ion etching (RIE). Then, the silicon slot PCW is first implanted with phosphorus ions at energy of 92keV and dose of 1.05×10^{12}/cm^2 to reach an ion concentration of 1×10^{17}cm^{-3}. Next, the device is patterned by photolithography and selectively implanted with phosphorus ions at energy of 92keV and dose of 1.05×10^{15}/cm^2 to reach an ion concentration of 1×10^{20}cm^{-3} in the region which will connect the gold electrodes in order to form ohmic contacts. A rapid thermal annealing at 1000°C for 10min in a flowing nitrogen environment is followed to remove the ion bombardment induced defects and activate the implanted ions, which also improves the optical performance of the ion-implanted waveguides. Next, 1μm-thick gold electrodes with

This article has been accepted for publication in a future issue of this journal, but has not been fully edited. Content may change prior to final publication. Citation information: DOI 10.1109/JLT.2015.2471853, Journal of Lightwave Technology

5nm-thick chromium adhesion layers are patterned using photolithography, electron-beam evaporation, and lift-off. Figures 3 (a) and (b) show the SEM images of the fabricated device. Figure 3 (c) shows a top view of the fabricated slot PCW, with arrows indicating the shifted lattices.

Next, the guest-host EO polymer is formulated and placed on an automatic roller to form a very viscous and homogeneous solution. The solution is then filtered through a 0.2μm poly(tetrafluoroethylene) (PTFE) filter and spincoated over the PCW and dispersed into the holes and slot. The EO polymer filled slot PCW device is then cured in a vacuum oven at 80℃ to get rid of possible air bubbles. Figure 3 (d) shows the cross section after EO polymer filling.

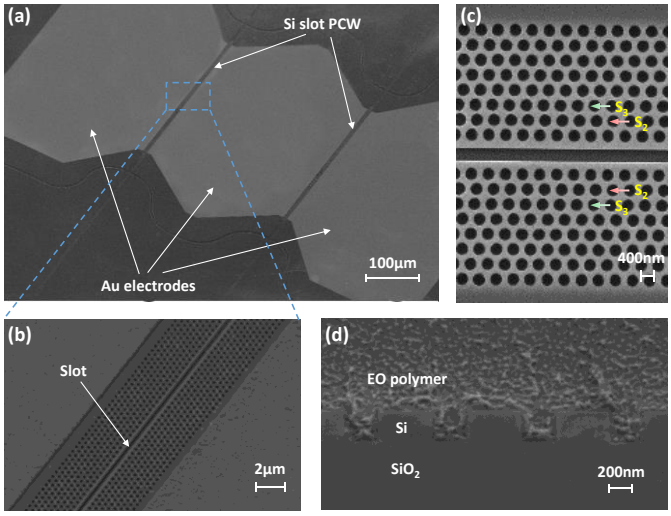

Fig. 3. SEM images of the fabricated device. (a) A tilted view of the symmetric MZI modulator with silicon slot PCWs in both arms. (b) A magnified image of the silicon slot PCW in one arm inside the gap of electrodes. (c) A top view of the slot PCW, with arrows indicating the shifted lattices on the second and third rows. S_2=-85nm, and S_3=85nm. (d) A cross-sectional view of the photonic crystal structure filled with EO polymer.

Finally, to activate the EO effect, a poling process is performed [45-47]. The device is heated up on a hot plate to the EO polymer glass transition temperature of 150℃ in a nitrogen atmosphere, and a constant poling electric field of 110V/μm is applied across the EO polymer inside the slot in a push-pull configuration, as shown in Fig. 1 (d). The randomly oriented chromophore dipoles inside the polymer matrix are then free to rotate and align in the direction of poling electric field. Next the temperature is quickly lowered to room temperature while the constant electric field is still applied, and eventually the chromophores are locked in a uniform direction to form a noncentrosymmetric structure. After the temperature decreases to room temperature, the poling electric field is then turned off. During The whole poling process, the leakage current is monitored and it remains below 0.53nA, corresponding to a low leakage current density of 5.5A/m^2. This is comparable to the typical leakage current density of 1-10A/m^2 measured in a thin film configuration, indicating a high poling efficiency [21].

IV. Characterization

A. Measuring modulation efficiency

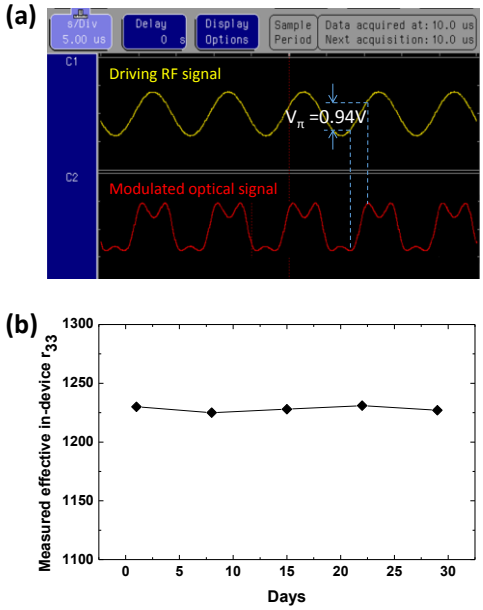

Fig. 4. Device characterization at low frequency. (a) Transfer function at 100kHz. The V_π is measured to be 0.94V from over-modulation. (b) Measured effective in-device r_{33} as a function of time in days, indicating the long-term stability of the modulator.

A low-frequency modulation test is first performed on the device to measure the voltage-length product, $V_\pi \times L$, which is a figure of merit (FOM) for optical modulators. TE-polarized light from a tunable laser source (1550nm) is coupled into and out of the device utilizing an in-house built grating coupler setup [33]. An RF signal from a function generator is applied onto the electrodes in a push-pull configuration, as shown in Fig. 1 (d). The modulator is biased at the 3dB point and driven by a sinusoidal RF wave with a peak-to-peak voltage of V_d=1.5V at 100KHz. The modulated output optical signal is detected using an amplified avalanche photodetector and a digital oscilloscope setup. As shown in Fig. 4 (a), over-modulation is observed on the output optical waveform, and the V_π of the modulator is measured to be 0.94V. Thus, the FOM of the modulator achieved is $V_\pi \times L$=0.94V×300μm=0.282V×mm at the frequency of 100KHz. The effective in-device r_{33} is then calculated using [8]

$$r_{33,eff} = \frac{\lambda S_w}{n^3 V_\pi \sigma L} = 1230 \text{ pm/V} \quad (1)$$

where λ=1550nm, S_w=320nm, n=1.63, L=300μm, and σ=0.33, which is the highest in-device r_{33} ever recorded. Such a high r_{33} value originates from the combined effects of a large bulk r_{33} of the EO polymer material, an improved poling efficiency achieved via widening the slot width (320nm), the slow-light enhancement in the silicon PCW, as well as the increased percentage of voltage drop across the slot due to silicon doping. Discounting the slow-light effect, the actual in-device r_{33} is estimated to be as high as 98pm/V [48-50]. Note that the

This article has been accepted for publication in a future issue of this journal, but has not been fully edited. Content may change prior to final publication. Citation information: DOI 10.1109/JLT.2015.2471853, Journal of Lightwave Technology

r_{33} value of EO polymer material does not change up to 100GHz or even higher RF frequency, while other parasitic elements may change. Furthermore, to verify the long-term stability of the device, the same test is repeated in the same conditions over the duration of a month, and the measured effective in-device r_{33} as a function of time in days is shown in Fig. 4 (b). It can be seen that no severe degradation of device performance is observed after a month, due to the good stability of the EO polymer material.

B. Measuring RF bandwidth

The RF bandwidth is measured in a small signal modulation test. RF driving signal is provided by a vector network analyzer (VNA) and applied onto the electrodes of the modulator via a ground-signal-ground (GSG) picoprobe. The modulated optical signal is amplified by an erbium doped fiber amplifier (EDFA) and received by a high-speed photodetector, and then the received power is measured using a microwave spectrum analyzer (MSA). The measurement system is calibrated using short-open-load technique. The measured EO response of the device as a function of modulation frequency is normalized to the response of the photodetector and shown in Fig. 5 (a), from which a 3-dB modulation bandwidth of 11GHz is measured. Note that the upper frequency of this measurement is limited by the upper limit of our MSA, which is 26GHz.

Next, in order to overcome this measurement limit and demonstrate the modulation response at frequencies over 26GHz, we perform another measurement using a sideband detection technique [51-54]. The optical output of the modulator is directly connected to the optical spectrum analyzer (OSA), and the transmission spectrum of the modulator is measured. When the modulator is driven by a high frequency RF signal, two sidebands appear in the transmission spectrum, equally spaced around the main peak [51, 52, 55, 53, 54]. Figure 5 (b) shows overlaid transmission spectra of the optical modulator driven at 10GHz, 20GHz, 30GHz and 40GHz. At higher modulation frequencies, the power of the sidebands becomes lower mainly due to the reduced slot impedance ($1/|j\omega C|$) which causes the decrease of voltage drop across the slot. Moreover, the skin effect also contributes to an increase in silicon resistance, which further reduces the voltage drop across the slot. The power of the main peak and first sideband is proportional to the square of the zero-order and first-order Bessel function of the first kind (J_i, i=0,1) as a function of phase modulation index (η). η represents the achieved phase shift (unit: radians). By measuring the ratio of the main peak power and sideband power $[J_0^2(\eta)/ J_1^2(\eta) \approx (2/\eta)^2]$, η can be extracted [22, 52, 55, 53]. The obtained η as a function of modulation frequency is plotted as the red curve shown in Fig. 5 (c). Sideband signals are observed above the noise floor until the modulation frequency is over 43GHz. The lower and upper limits of the frequency range are limited by the resolution bandwidth of the OSA and by the maximum frequency of VNA.

C. Characterizing improved RF bandwidth under backside gate voltage.

Next, to further increase the RF bandwidth of the modulator, a positive gate voltage (V_{gate}) from a high-voltage supply is applied to the bottom silicon substrate across the BOX layer of our device [22, 23], as shown in Fig. 1 (d). The positive V_{gate} is varied from 0V to 300V, and the corresponding modulation index is measured. As shown in Fig. 5 (c), as the positive V_{gate} increases, the measured modulation index at each frequency increases and the whole curve becomes flatter, due to the increased electron accumulation at the interface of the silicon PCW and the BOX [22, 23]. When the V_{gate} is increased over 150V, the sideband power starts to appear above the noise level in the transmission spectrum at even 50GHz and the corresponding modulation index is plotted the blue curve shown in Fig. 5 (c). Further increasing the positive gate voltage, e.g. up to 300V, helps improving the modulation index at the same frequency, or extending the RF frequency with the same modulation index, as shown by the green curve in Fig. 5 (c). Figure 5 (d) shows the 3-dB bandwidth of the modulator as a function of positive V_{gate}, and it can be seen that under the V_{gate} of 300V, the 3-dB bandwidth is increased to 15GHz. Note the breakdown electric field of the silicon dioxide is about 0.5GV/m [56], corresponding to a voltage of 1500V that the 3μm-thick BOX layer can withstand.

In order to further investigate the device performance under V_{gate}, a negative V_{gate} is applied, and the modulation index (η) is measured and plotted in Fig. 5 (e). It can be seen that with the voltage slightly changed from 0V to -75V, the measured η decreases due to the depletion of electrons. At a V_{gate} of around -75V, the free electrons are almost completely depleted, so η becomes the smallest, which is shown by the black curve in Fig. 5 (c). When the magnitude of the negative voltage further increases, η starts to increase because "inversion" state occurs in which holes are accumulated in the top silicon PCW layer. This interesting phenomenon is quite similar to the well-known Metal-Oxide-Semiconductor (MOS) capacitor structure [57].

D. Estimating power consumption

What is more, a small switching voltage is achieved under a high positive V_{gate}, suggesting a low power consumption. For example, the measured modulation index is η=0.23 at 10GHz under V_{gate}=300V, and correspondingly, the required switching voltage is then $V_\pi = \pi/\eta \times V_d$ =2.2V at 10GHz, where V_d= 0.16V is the RF driving voltage measured across a 50ohm resistor from the output power of RF source. With this V_π=2.2V at 10GHz, the corresponding $V_\pi \times L$ and effective in-device r_{33} measured at 10GHz are then 0.66V×mm and 526pm/V, respectively. Compared with the values measured at 100KHz, the V_π is increased and effective in-device r_{33} is decreased at 10GHz. This is mainly because of the reduced impedance in the slot ($1/|j\omega C|$) at high frequencies and also the increased impedance in the silicon PCW due to skin effect, which cause the decrease of voltage drop across the slot. Note that the r_{33} of the EO polymer material does not change up to 100GHz or even higher RF frequency.

Since our modulator is a lumped device without termination, the power consumption is then dominated by the capacitive load of the slot. The estimated RF power consumption for

This article has been accepted for publication in a future issue of this journal, but has not been fully edited. Content may change prior to final publication. Citation information: DOI 10.1109/JLT.2015.2471853, Journal of Lightwave Technology

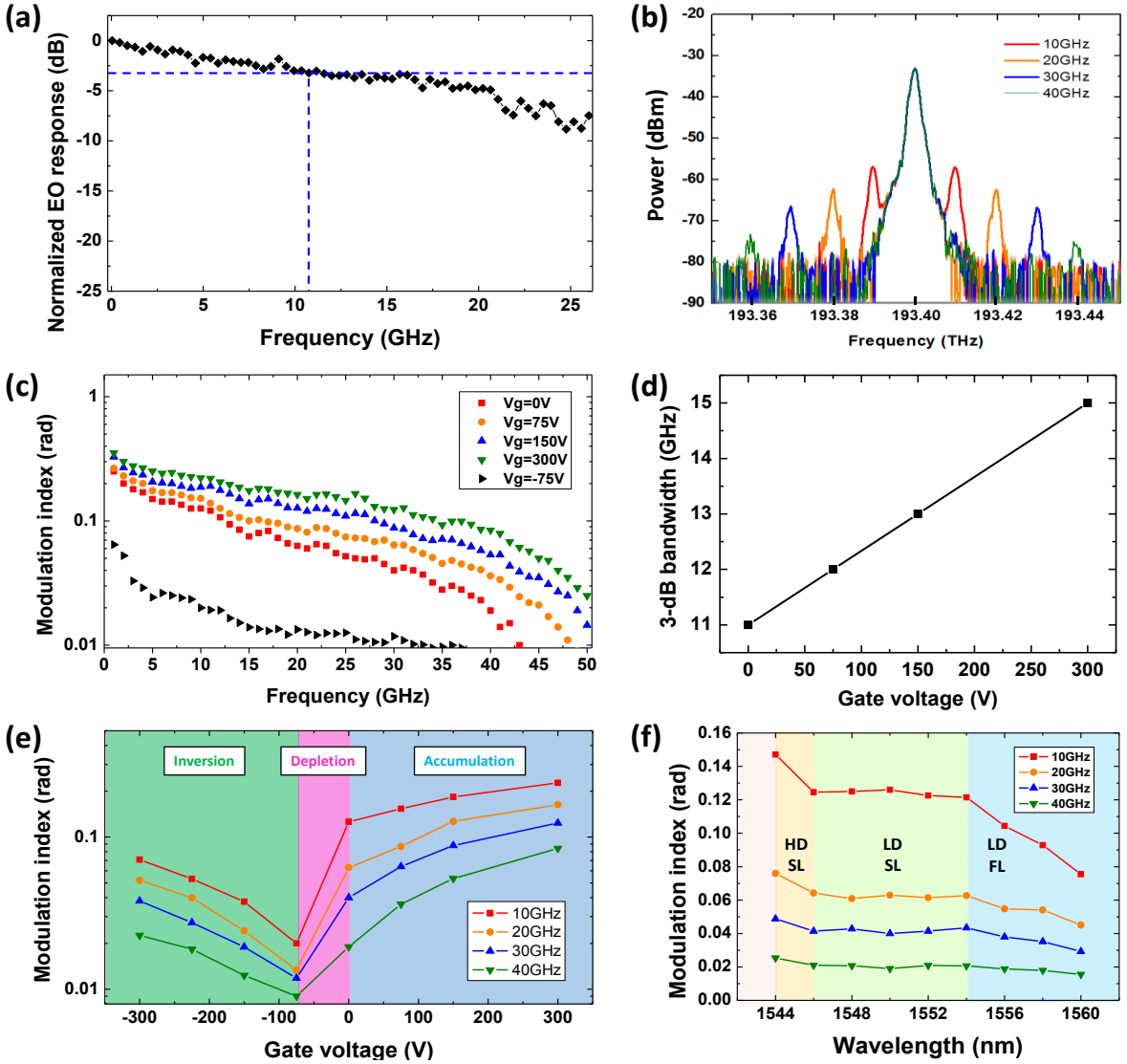

Fig. 5. Device characterization at high frequency. (a) Measured normalized EO response of the modulator as a function of RF frequency in a small-signal modulation test. The 3-dB modulation bandwidth is measured to be 11GHz. (b) Measured optical transmission spectra of the modulator operating at 10GHz, 20GHz, 30GHz and 40GHz. (c) Measured modulation index as a function of frequency, under different backside gate voltages. (d) Increased 3-dB RF bandwidth as the positive gate voltage increases. (e) Measured modulation index as a function of V_{gate} at different modulation frequencies, overlaid with the states of accumulation, depletion and inversion. (f) Measured modulation index over a range of optical wavelengths. The modulation index is nearly constant over a low-dispersion slow-light region of 8nm.

100% modulation depth is $2\pi f \times (\frac{1}{2} CV_\pi^2) \times 2$=24mW at modulation frequency of f=10GHz, where C=39fF is the slot capacitance obtained from simulation and verified experimentally, V_π=2.2V is used as the driving voltage to achieve a maximum extinction ratio, and a factor of 2 is added due to the push-pull configuration. In addition, we make an estimation of energy consumption per bit for our device [58]. If our modulator is driven by pseudo-random binary sequence (PRBS) signals with the same power level, we estimate the energy consumption per bit for our modulator at the bit rate of 10Gbit/s as $W_{bit} = \frac{1}{4} CV_\pi^2 \times 2$ = 94.4fJ/bit [59, 58, 60, 3, 23, 53]. Note that, in actual high-speed digital modulations, the driving voltage can be smaller than V_π, in which case a decently clear eye diagram, a high enough extinction ratio and acceptable bit error rate (BER) can be still achieved using lower energy [24, 18, 61, 62, 23]. Though, we still use V_π as driving voltage (i.e.100% modulation depth) in our estimation, because this can compensate the actual voltage drop caused by experimental imperfections such as reflections, drift, RF loss, etc., and allows for a reasonable estimated value of energy consumption. The very low power/energy consumption is due to both a significantly reduced V_π and the very small capacitance achieved by widening the slot. Note that, although the applied V_{gate} is high, the power consumption on the backside gate is negligible (<30pW) due to the highly insulating BOX layer.

E. Demonstrating low-dispersion spectrum range

Finally, to demonstrate the wide optical bandwidth of this PCW modulator, the wavelength of the laser input (TE

This article has been accepted for publication in a future issue of this journal, but has not been fully edited. Content may change prior to final publication. Citation information: DOI 10.1109/JLT.2015.2471853, Journal of Lightwave Technology

polarized) is tuned from 1544nm to 1560nm, while V_{gate} is set to be zero and all other testing conditions are kept the same. Over this spectrum range, the modulation index is measured at 10GHz, 20GHz, 30GHz, and 40GHz, and the results are plotted in Fig. 5 (f). It can be seen that at each modulation frequency, the curve of the measured modulation index looks flat from 1546nm to 1554nm, with a small variation of ±3.5%. This is because the modulation index is proportional to the n_g ($\eta \sim 1/V_\pi$ and $V_\pi \sim B\times\lambda/n_g$, where B is a constant) [63], and n_g has been engineered to be almost constant in this slow-light wavelength region, which agrees well with the simulated low-dispersion spectrum range in Fig. 1 (c). This 8nm-wide low-dispersion spectrum range is over an order of magnitude wider than that in non-band-engineered PCWs [7, 24] and ring resonators [25, 64-66], so it makes our modulator insensitive to variations of wavelength and temperature. This is also promising for applications such as dense wavelength division multiplexing (DWDM) in optical interconnects and networks. In Fig. 5 (f), the largest modulation index is achieved in the high-dispersion slow-light region (from 1543.5nm to 1546 nm), because of the largest n_g in this region. As the wavelength increases over 1554nm, the measured modulation index decreases due to the decreasing value of n_g.

V. Discussion

In recent years, some groups have reported their work on analog/digital optical modulators based on similar structures such as silicon PCW MZI [18] and EO polymer filled silicon slot waveguide MZI [23], while our EO polymer filled silicon slot PCW MZI modulator combines the benefits from both the slow-light PCW [18] and the silicon-organic hybrid (SOH) structure [23]. In Reference [18], Nguyen, et al, demonstrated a silicon Mach-Zehnder modulators with 90μm-long lattice-shifted photonic crystal waveguides with n_g=20~30. By utilizing the plasma dispersion effect on p-n diode, digital modulation at a data rate of 40Gbit/s, optical bandwidth of 12.5nm, and insertion loss of 14.8dB were experimentally demonstrated. Since only a peak-to-peak driving voltage, V_{pp}=5.3V (instead of V_π), is reported in this reference, we theoretically estimate the V_π of the modulator [34, 63, 67] to be

$$V_\pi = \pi \Big/ \left(\frac{2\pi}{\lambda}\Delta n_{eff} n_g L\right) = \pi \Big/ \left(\frac{2\pi}{1550nm}\cdot 1.6\times 10^{-5}\cdot 30\cdot 90\mu m\right)$$

=18V for apples-to-apples comparison. This large V_π value leads to a large $V_\pi\times L$ product of 1.62V×mm at 10Gbit/s. In reference [23], Palmer, et al, reported a MZI modulator in which EO polymer is filled into a 1.5mm-long slot waveguide with slot width of 80nm. This modulator was demonstrated with in-device r_{33} of 15pm/V, energy consumption of 320fJ/bit at 10Gbit/s digital modulation, total insertion loss of 21dB, and V_π=2.5V which corresponds to a $V_\pi\times L$=3.75V×mm. In a recent article published by the same group [68], Alloatti, et al, demonstrated a MZI modulator with 500μm-long 120nm-wide-slot waveguide filled with EO polymer, in which they reported a 3dB bandwidth of 100GHz, but a relatively higher $V_\pi\times L$=11V×mm, as well as optical loss of 21±2dB. In addition, recently, a rather specialized SOH modulator based on plasmonic waveguide has been demonstrated by Melikyan, et al, with bit rate of 40Gbit/s, energy consumption of 60fJ/bit, optical bandwidth of 120nm, and insertion loss of 12dB [53]. Considering the reported $V_\pi\times L$=1.3Vmm and device length of 29um, its value of V_π is as large as 45V, which may be prohibitive for some applications.

Besides, the fiber-to-fiber total optical insertion loss of our device is estimated to be 15dB, including the ~3.5dB loss per grating coupler, ~0.4dB loss per MMI coupler, ~0.1dB loss per mode converter, ~0.5dB loss per group index taper, and ~6dB insertion loss on EO polymer filled slot PCW, based on CMOS foundry fabrication conditions [69]. In our measurements, we observed a higher insertion loss, and the additional losses can be mainly dominated by the imperfect fabrication quality (e.g. sidewall roughness) from our university fabrication tools. This abovementioned value is provided instead of the actual measured insertion loss in order to avoid misleading information about the true performance behavior of our device. The optical loss can be further reduced by the design of a low-loss slot PCW and passive components, improved fabrication quality, and improved coupling and packaging methods [70]. By using a mature commercial CMOS foundry to fabricate our PCW devices [69], the optical loss and fabrication yield can be improved.

VI. Conclusion

In summary, we demonstrate a high-speed, low-power, low-dispersion and compact optical modulator based on a silicon slot PCW filled with EO polymer. Benefiting from the combined enhancement provided by the slow-light effect in the PCW and the high r_{33} of the EO polymer, the voltage-length product of the modulator is measured to be as small as $V_\pi\times L$=0.282V×mm at 100KHz, corresponding to a record-high effective in-device r_{33} of 1230pm/V ever demonstrated. Excluding the slow-light effect, the actual in-device r_{33} is estimated to be as high as 98pm/V. The silicon PCW is selectively doped to reduce the RC time delay for high-speed modulation. A backside gate technique is applied to our silicon PCW device to enhance device performance. Assisted by the backside gate voltage of 300V, a modulation response up to 50GHz is observed, with the measured 3-dB bandwidth of 15GHz. In addition, the power consumption of the modulator is estimated to be 24mW at 10GHz, and the estimated value of energy consumption per bit for a potential digital modulation is approximately 94.4fJ/bit at 10Gbit/s based on measured V_π at 10GHz [58, 60, 3, 23, 53]. By using the band-engineered PCWs, the modulator is demonstrated to have a low-dispersion optical spectrum range as wide as 8nm, which is a factor of ~10X better than other modulators based on non-band-engineered PCWs [7, 24] and ring resonators [25] which have narrow operating optical bandwidth of <1 nm.

In our future work, the optical loss can be further reduced by the design of a low-loss slot PCW and passive components, improved fabrication quality, and improved coupling and packaging methods [70]. By using a mature commercial CMOS foundry to fabricate our PCW devices [69], the optical loss and fabrication yield can be improved. The $V_\pi\times L$ product can be further reduced by using more efficient organic EO materials, such as supramolecular organic EO glasses and

This article has been accepted for publication in a future issue of this journal, but has not been fully edited. Content may change prior to final publication. Citation information: DOI 10.1109/JLT.2015.2471853, Journal of Lightwave Technology

binary EO polymers exhibiting intrinsic Pockels coefficients greater than 300 pm/V [71, 72]. Very recently, an ultrahigh r_{33} value of 273 pm/V and high refractive index of 2.12 at the wavelength of 1300 nm have been achieved from monolithic glass, which represents a record-high n^3r_{33} figure-of-merit of 2601 pm/V with good temporal stability at 80℃ [72]. To further investigate the high-speed behavior limited by the RC constant, detailed values of the resistance and capacitance in the equivalent circuit model over the whole frequency band can be extracted by measuring the complex frequency-dependent amplitude reflection factor S11 at the device input using a VNA and then curve-fitting the measured S11 data [73, 64, 74]. And also, a transmission line could be designed to drive the modulator as a traveling wave device, in order to achieve modulation frequency over 100GHz [46, 75, 68, 76]. Recently, the SOH slot waveguide structures have been developed for digital modulations more advanced modulation formats such as QPSK and 16QAM at >1Tb/s [77, 78], thus, our future work will also include driving our modulator using high-speed digital signals [24, 18, 61] and also using this modulator for advanced modulation formats and coherent modulation scheme [77, 78]. The modulator can also enable an integrated transmitter via the hybrid integration with a laser diode and CMOS drivers on a polymer board for in data communication and telecommunication applications [79, 80]. And also, some other modulator parameters such as chirp characteristics will be investigated, and the small signal chirp parameter can be obtained by measuring the EO response by inserting a dispersive fiber between the modulator and the lightwave component analyzer (LCA) [81]. In addition, potential stability of the modulator, a common issue for almost all polymer based devices, can be further improved by developing new EO polymers with higher glass transition temperatures and crosslinking chemistry, and by hermetically sealing the EO polymer and removing oxygen in the device packaging [82]. More detailed studies of EO polymer thermal stability indicate that operation up to 150℃ results in a change of EO coefficients < 10% [83, 84].

ACKNOWLEDGMENT

The authors would like to acknowledge the Air Force Research Laboratory (AFRL) for supporting this work under the Small Business Technology Transfer Research (STTR) program (Grant No. FA8650-14-C-5006).

REFERENCES

[1] V. R. Almeida, Q. Xu, C. A. Barrios, and M. Lipson, "Guiding and confining light in void nanostructure," *Optics letters*, vol. 29, pp. 1209-1211, 2004.

[2] C. Koos, P. Vorreau, T. Vallaitis, P. Dumon, W. Bogaerts, R. Baets, B. Esembeson, I. Biaggio, T. Michinobu, F. Diederich, W. Freude, and J. Leuthold, "All-optical high-speed signal processing with silicon–organic hybrid slot waveguides," *Nature Photonics*, vol. 3, pp. 216-219, 2009.

[3] J. Leuthold, C. Koos, W. Freude, L. Alloatti, R. Palmer, D. Korn, J. Pfeifle, M. Lauermann, R. Dinu, S. Wehrli, M. Jazbinsek, P. Gunter, M. Waldow, T. Wahlbrink, J. Bolten, H. Kurz, M. Fournier, J.-M. Fedeli, H. Yu, and W. Bogaerts, "Silicon-organic hybrid electro-optical devices," *Selected Topics in Quantum Electronics, IEEE Journal of*, vol. 19, pp. 3401413-3401413, 2013.

[4] J. Takayesu, M. Hochberg, T. Baehr-Jones, E. Chan, G. Wang, P. Sullivan, Y. Liao, J. Davies, L. Dalton, A. Scherer, and W. Krug, "A Hybrid Electrooptic Microring Resonator-Based 1×4×1 ROADM for Wafer Scale Optical Interconnects," *Journal of Lightwave Technology*, vol. 27, pp. 440-448, 2009.

[5] X. Zhang, A. Hosseini, X. Lin, H. Subbaraman, and R. T. Chen, "Polymer-based Hybrid Integrated Photonic Devices for Silicon On-chip Modulation and Board-level Optical Interconnects," *IEEE Journal of Selected Topics in Quantum Electronics*, vol. 19, pp. 196-210, 2013.

[6] J.-M. Brosi, C. Koos, L. C. Andreani, M. Waldow, J. Leuthold, and W. Freude, "High-speed low-voltage electro-optic modulator with a polymer-infiltrated silicon photonic crystal waveguide," *Optics Express*, vol. 16, pp. 4177-4191, 2008.

[7] J. H. Wülbern, J. Hampe, A. Petrov, M. Eich, J. Luo, A. K.-Y. Jen, A. Di Falco, T. F. Krauss, and J. Bruns, "Electro-optic modulation in slotted resonant photonic crystal heterostructures," *Applied Physics Letters*, vol. 94, p. 241107, 2009.

[8] X. Zhang, A. Hosseini, H. Subbaraman, S. Wang, Q. Zhan, J. Luo, A. K. Jen, and R. T. Chen, "Integrated Photonic Electromagnetic Field Sensor Based on Broadband Bowtie Antenna Coupled Silicon Organic Hybrid Modulator," *Lightwave Technology, Journal of*, vol. 32, pp. 3774-3784, 2014.

[9] D. Chen, H. R. Fetterman, A. Chen, W. H. Steier, L. R. Dalton, W. Wang, and Y. Shi, "Demonstration of 110 GHz electro-optic polymer modulators," *Applied Physics Letters*, vol. 70, pp. 3335-3337, 1997.

[10] R. T. Chen, L. Lin, C. Choi, Y. J. Liu, B. Bihari, L. Wu, S. Tang, R. Wickman, B. Picor, M. Hibb-Brenner, J. Bristow, and Y. S. Liu, "Fully embedded board-level guided-wave optoelectronic interconnects," *Proceedings of the IEEE*, vol. 88, pp. 780-793, 2000.

[11] Y. Shi, C. Zhang, H. Zhang, J. H. Bechtel, L. R. Dalton, B. H. Robinson, and W. H. Steier, "Low (sub-1-volt) halfwave voltage polymeric electro-optic modulators achieved by controlling chromophore shape," *Science*, vol. 288, pp. 119-122, 2000.

[12] X. Lin, T. Ling, H. Subbaraman, X. Zhang, K. Byun, L. J. Guo, and R. T. Chen, "Ultraviolet imprinting and aligned ink-jet printing for multilayer patterning of electro-optic polymer modulators," *Optics letters*, vol. 38, pp. 1597-1599, 2013.

[13] R. Soref, "The past, present, and future of silicon photonics," *Selected Topics in Quantum Electronics, IEEE Journal of*, vol. 12, pp. 1678-1687, 2006.

[14] G. T. Reed, G. Mashanovich, F. Gardes, and D. Thomson, "Silicon optical modulators," *Nature Photonics*, vol. 4, pp. 518-526, 2010.

[15] Y. A. Vlasov, M. O'Boyle, H. F. Hamann, and S. J. McNab, "Active control of slow light on a chip with photonic crystal waveguides," *Nature*, vol. 438, pp. 65-69, 2005.

[16] T. Baba, "Slow light in photonic crystals," *Nature Photonics*, vol. 2, pp. 465-473, 2008.

[17] Y. Jiang, W. Jiang, L. Gu, X. Chen, and R. T. Chen, "80-micron interaction length silicon photonic crystal waveguide modulator," *Applied Physics Letters*, vol. 87, p. 221105, 2005.

[18] H. C. Nguyen, S. Hashimoto, M. Shinkawa, and T. Baba, "Compact and fast photonic crystal silicon optical modulators," *Optics Express*, vol. 20, pp. 22465-22474, 2012.

[19] C.-Y. Lin, X. Wang, S. Chakravarty, B. S. Lee, W. Lai, J. Luo, A. K.-Y. Jen, and R. T. Chen, "Electro-optic polymer infiltrated silicon photonic crystal slot waveguide modulator with 23 dB slow light enhancement," *Applied Physics Letters*, vol. 97, p. 093304, 2010.

[20] X. Wang, C.-Y. Lin, S. Chakravarty, J. Luo, A. K.-Y. Jen, and R. T. Chen, "Effective in-device r33 of 735 pm/V on electro-optic polymer infiltrated silicon photonic crystal slot waveguides," *Optics letters*, vol. 36, pp. 882-884, 2011.

[21] X. Zhang, A. Hosseini, S. Chakravarty, J. Luo, A. K.-Y. Jen, and R. T. Chen, "Wide optical spectrum range, subvolt, compact modulator based on an electro-optic polymer refilled silicon slot photonic crystal waveguide," *Optics letters*, vol. 38, pp. 4931-4934, 2013.

[22] L. Alloatti, D. Korn, R. Palmer, D. Hillerkuss, J. Li, A. Barklund, R. Dinu, J. Wieland, M. Fournier, J. Fedeli, H. Yu, W. Bogaerts, P. Dumon, R. Baets, C. Koos, W. Freude, and J. Leuthold, "42.7 Gbit/s electro-optic modulator in silicon technology," *Optics Express*, vol. 19, pp. 11841-11851, 2011.

[23] R. Palmer, A. Luca, D. Korn, P. Schindler, M. Baier, J. Bolten, T. Wahlbrink, M. Waldow, R. Dinu, W. Freude, C. Koos, and J. Leuthold,

"Low power mach-zehnder modulator in silicon-organic hybrid technology," *Photonics Technology Letters, IEEE*, vol. 25, 2013.

[24] H. C. Nguyen, Y. Sakai, M. Shinkawa, N. Ishikura, and T. Baba, "10 Gb/s operation of photonic crystal silicon optical modulators," *Optics Express*, vol. 19, pp. 13000-13007, 2011.

[25] M. Gould, T. Baehr-Jones, R. Ding, S. Huang, J. Luo, A. K.-Y. Jen, J.-M. Fedeli, M. Fournier, and M. Hochberg, "Silicon-polymer hybrid slot waveguide ring-resonator modulator," *Optics Express*, vol. 19, pp. 3952-3961, 2011.

[26] S. Huang, T.-D. Kim, J. Luo, S. K. Hau, Z. Shi, X.-H. Zhou, H.-L. Yip, and A. K.-Y. Jen, "Highly efficient electro-optic polymers through improved poling using a thin TiO 2-modified transparent electrode," *Applied Physics Letters*, vol. 96, pp. 243311-243311-3, 2010.

[27] H. Chen, B. Chen, D. Huang, D. Jin, J. Luo, A.-Y. Jen, and R. Dinu, "Broadband electro-optic polymer modulators with high electro-optic activity and low poling induced optical loss," *Applied Physics Letters*, vol. 93, p. 043507, 2008.

[28] T. Baehr-Jones, B. Penkov, J. Huang, P. Sullivan, J. Davies, J. Takayesu, J. Luo, T.-D. Kim, L. Dalton, and A. Jen, "Nonlinear polymer-clad silicon slot waveguide modulator with a half wave voltage of 0.25 V," *Applied Physics Letters*, vol. 92, p. 163303, 2008.

[29] J. Blasco and C. Barrios, "Compact slot-waveguide/channel-waveguide mode-converter," in *Lasers and Electro-Optics Europe, 2005. CLEO/Europe. 2005 Conference on*, 2005, pp. 607-607.

[30] R. Palmer, A. Luca, D. Korn, W. Heni, P. Schindler, J. Bolten, M. Karl, M. Waldow, T. Wahlbrink, W. Freude, K. C, and L. J, "Low-loss silicon strip-to-slot mode converters," *IEEE Photonics Journal*, 2013.

[31] X. Zhang, H. Subbaraman, A. Hosseini, and R. T. Chen, "Highly efficient mode converter for coupling light into wide slot photonic crystal waveguide," *Optics Express*, vol. 22, pp. 20678-20690, 2014.

[32] A. Hosseini, X. Xu, D. N. Kwong, H. Subbaraman, W. Jiang, and R. T. Chen, "On the role of evanescent modes and group index tapering in slow light photonic crystal waveguide coupling efficiency," *Applied Physics Letters*, vol. 98, pp. 031107-031107-3, 2011.

[33] X. Xu, H. Subbaraman, J. Covey, D. Kwong, A. Hosseini, and R. T. Chen, "Complementary metal–oxide–semiconductor compatible high efficiency subwavelength grating couplers for silicon integrated photonics," *Applied Physics Letters*, vol. 101, pp. 031109-031109-4, 2012.

[34] M. Soljačić, S. G. Johnson, S. Fan, M. Ibanescu, E. Ippen, and J. Joannopoulos, "Photonic-crystal slow-light enhancement of nonlinear phase sensitivity," *JOSA B*, vol. 19, pp. 2052-2059, 2002.

[35] C. M. Kim and R. V. Ramaswamy, "Overlap integral factors in integrated optic modulators and switches," *Lightwave Technology, Journal of*, vol. 7, pp. 1063-1070, 1989.

[36] J. Witzens, T. Baehr-Jones, and M. Hochberg, "Design of transmission line driven slot waveguide Mach-Zehnder interferometers and application to analog optical links," *Optics Express*, vol. 18, pp. 16902-16928, 2010.

[37] J. H. WŘlbern, A. Petrov, and M. Eich, "Electro-optical modulator in a polymerinfiltrated silicon slotted photonic crystal waveguide heterostructure resonator," *Optics Express*, vol. 17, pp. 304-313, 2009.

[38] S. K. Ghandhi, *VLSI fabrication principles: silicon and gallium arsenide*: John Wiley & Sons, 2008.

[39] A. Chen, H. Sun, A. Szep, S. Shi, D. Prather, Z. Lin, R. S. Kim, and D. Abeysinghe, "Achieving higher modulation efficiency in electrooptic polymer modulator with slotted silicon waveguide," *Lightwave Technology, Journal of*, vol. 29, pp. 3310-3318, 2011.

[40] J. Doylend, P. Jessop, and A. Knights, "Optical attenuation in ion-implanted silicon waveguide racetrack resonators," *Opt. Express19 (16)*, pp. 14913-14918, 2011.

[41] S. Ristić, A. Prijić, and Z. Prijić, "Dependence of static dielectric constant of silicon on resistivity at room temperature," *Serbian Journal of Electrical Engineering*, vol. 1, pp. 237-247, 2004.

[42] W. Perrins, D. McKenzie, and R. McPhedran, "Transport properties of regular arrays of cylinders," *Proceedings of the Royal Society of London. A. Mathematical and Physical Sciences*, vol. 369, pp. 207-225, 1979.

[43] T. C. Choy, *Effective medium theory: principles and applications*: Oxford University Press, 1999.

[44] L. Alloatti, M. Lauermann, C. Sürgers, C. Koos, W. Freude, and J. Leuthold, "Optical absorption in silicon layers in the presence of charge inversion/accumulation or ion implantation," *Applied Physics Letters*, vol. 103, p. 051104 2013.

[45] C.-Y. Lin, A. X. Wang, B. S. Lee, X. Zhang, and R. T. Chen, "High dynamic range electric field sensor for electromagnetic pulse detection," *Optics Express*, vol. 19, pp. 17372-17377, 2011.

[46] X. Zhang, B. Lee, C.-y. Lin, A. X. Wang, A. Hosseini, and R. T. Chen, "Highly Linear Broadband Optical Modulator Based on Electro-Optic Polymer," *Photonics Journal, IEEE*, vol. 4, pp. 2214-2228, 2012.

[47] X. Zhang, A. Hosseini, J. Luo, A. K.-Y. Jen, and R. T. Chen, "Hybrid silicon-electro-optic-polymer integrated high-performance optical modulator," in *SPIE Photonic West, OPTO*, 2014, pp. 89910O-89910O-6.

[48] T. F. Krauss, "Slow light in photonic crystal waveguides," *Journal of Physics D: Applied Physics*, vol. 40, p. 2666, 2007.

[49] A. Hosseini, X. Xu, H. Subbaraman, C.-Y. Lin, S. Rahimi, and R. T. Chen, "Large optical spectral range dispersion engineered silicon-based photonic crystal waveguide modulator," *Opt. Express20 (11)*, pp. 12318-12325, 2012.

[50] S.-i. Inoue and A. Otomo, "Electro-optic polymer/silicon hybrid slow light modulator based on one-dimensional photonic crystal waveguides," *Applied Physics Letters*, vol. 103, p. 171101, 2013.

[51] J. H. Wülbern, S. Prorok, J. Hampe, A. Petrov, M. Eich, J. Luo, A. K.-Y. Jen, M. Jenett, and A. Jacob, "40 GHz electro-optic modulation in hybrid silicon–organic slotted photonic crystal waveguides," *Optics letters*, vol. 35, pp. 2753-2755, 2010.

[52] Y. N. Wijayanto, H. Murata, and Y. Okamura, "Electro-optic microwave-lightwave converters utilizing patch antennas with orthogonal gaps," *Journal of Nonlinear Optical Physics & Materials*, vol. 21, 2012.

[53] A. Melikyan, L. Alloatti, A. Muslija, D. Hillerkuss, P. Schindler, J. Li, R. Palmer, D. Korn, S. Muehlbrandt, D. Van Thourhout, B. Chen, R. Dinu, M. Sommer, C. Koos, M. Kohl, W. Freude, and J. Leuthold, "High-speed plasmonic phase modulators," *Nature Photonics*, vol. 8, pp. 229-233, 2014.

[54] L. D. Tzuang, M. Soltani, Y. H. D. Lee, and M. Lipson, "High RF carrier frequency modulation in silicon resonators by coupling adjacent free-spectral-range modes," *Optics letters*, vol. 39, pp. 1799-1802, 2014.

[55] O. D. Herrera, K.-J. Kim, R. Voorakaranam, R. Himmelhuber, S. Wang, V. Demir, Q. Zhan, L. Li, R. A. Norwood, R. L. Nelson, J. Luo, A. K. Y. Jen, and N. Peyghambarian, "Silica/Electro-Optic Polymer Optical Modulator With Integrated Antenna for Microwave Receiving," *Journal of Lightwave Technology*, vol. 32, pp. 3861-3867, 2014/10/15 2014.

[56] H. Bartzsch, D. Glöß, P. Frach, M. Gittner, E. Schultheiß, W. Brode, and J. Hartung, "Electrical insulation properties of sputter-deposited SiO2, Si3N4 and Al2O3 films at room temperature and 400 °C," *Physica Status Solidi (A)*, vol. 206, pp. 514-519, 2009.

[57] S. M. Sze and K. K. Ng, *Physics of semiconductor devices*: John Wiley & Sons, 2006.

[58] D. A. Miller, "Energy consumption in optical modulators for interconnects," *Optics Express*, vol. 20, pp. A293-A308, 2012.

[59] X. Chen, Y.-S. Chen, Y. Zhao, W. Jiang, and R. T. Chen, "Capacitor-embedded 0.54 pJ/bit silicon-slot photonic crystal waveguide modulator," *Optics letters*, vol. 34, pp. 602-604, 2009.

[60] J. Leuthold, C. Koos, W. Freude, L. Alloatti, R. Palmer, D. Korn, J. Pfeifle, M. Lauermann, R. Dinu, S. Wehrli, M. Jazbinsek, P. Gunter, M. Waldow, T. Wahlbrink, J. Bolten, M. Fournier, J. M. Fedeli, W. Bogaerts, and H. Yu, "High-speed, low-power optical modulators in silicon," in *Transparent Optical Networks (ICTON), 2013 15th International Conference on*, 2013, pp. 1-4.

[61] H. C. Nguyen, Y. Sakai, M. Shinkawa, N. Ishikura, and T. Baba, "Photonic crystal silicon optical modulators: carrier-injection and depletion at 10 Gb/s," *Quantum Electronics, IEEE Journal of*, vol. 48, pp. 210-220, 2012.

[62] R. Palmer, S. Koeber, W. Heni, D. Elder, D. Korn, H. Yu, L. Alloatti, S. Koenig, P. Schindler, W. Bogaerts, L. Dalton, W. Freude, J. Leuthold, and C. Koos, "High-speed silicon-organic hybrid (SOH) modulator with 1, 6 fJ/bit and 180 pm/V in-device nonlinearity," in *39th European Conference and Exhibition on Optical Communication (ECOC-2013)*, 2013.

[63] A. Hosseini, X. Xu, H. Subbaraman, C.-Y. Lin, S. Rahimi, and R. T. Chen, "Large optical spectral range dispersion engineered silicon-based

photonic crystal waveguide modulator," *Opt. Express*, vol. 20, pp. 12318-12325, 2012.

[64] L. Chen, Q. Xu, M. G. Wood, and R. M. Reano, "Hybrid silicon and lithium niobate electro-optical ring modulator," *Optica*, vol. 1, pp. 112-118, 2014.

[65] C. Xiong, W. H. Pernice, J. H. Ngai, J. W. Reiner, D. Kumah, F. J. Walker, C. H. Ahn, and H. X. Tang, "Active silicon integrated nanophotonics: ferroelectric BaTiO3 devices," *Nano letters*, vol. 14, pp. 1419-1425, 2014.

[66] C. Zhang, T. Ling, S.-L. Chen, and L. J. Guo, "Ultrabroad Bandwidth and Highly Sensitive Optical Ultrasonic Detector for Photoacoustic Imaging," *ACS Photonics*, 2014.

[67] Y. Terada and T. Baba, "Low-Voltage 25 Gbps Modulators Based On Si Photonic Crystal Slow Light Waveguides," in *CLEO: Science and Innovations*, 2014, p. SM2G. 2.

[68] L. Alloatti, R. Palmer, S. Diebold, K. P. Pahl, B. Q. Chen, R. Dinu, M. Fournier, J. M. Fedeli, T. Zwick, W. Freude, C. Koos, and J. Leuthold, "100 GHz silicon-organic hybrid modulator," *Light-Science & Applications*, vol. 3, May 2014.

[69] E. Schelew, G. W. Rieger, and J. F. Young, "Characterization of integrated planar photonic crystal circuits fabricated by a CMOS foundry," *Lightwave Technology, Journal of*, vol. 31, pp. 239-248, 2013.

[70] B. Snyder and P. O'Brien, "Planar fiber packaging method for silicon photonic integrated circuits," in *Optical Fiber Communication Conference and Exposition (OFC/NFOEC) 2012*, 2012, pp. 1-3.

[71] R. Palmer, S. Koeber, D. L. Elder, M. Woessner, W. Heni, D. Korn, M. Lauermann, W. Bogaerts, L. Dalton, W. Freude, J. Leuthold, and C. Koos, "High-Speed, Low Drive-Voltage Silicon-Organic Hybrid Modulator Based on a Binary-Chromophore Electro-Optic Material," *Journal of Lightwave Technology*, vol. 32, pp. 2726-2734, 2014.

[72] M. Li, S. Huang, X.-H. Zhou, Y. Zang, J. Wu, Z. Cui, J. Luo, and A. K. Jen, "Poling Efficiency Enhancement of Tethered Binary Nonlinear Optical Chromophores for Achieving Ultrahigh n3r33 Figure-of-Merit of 2601 pm/V," *Journal of Materials Chemistry C*, 2015.

[73] G. Li, X. Zheng, J. Yao, H. Thacker, I. Shubin, Y. Luo, K. Raj, J. E. Cunningham, and A. V. Krishnamoorthy, "25Gb/s 1V-driving CMOS ring modulator with integrated thermal tuning," *Optics Express*, vol. 19, pp. 20435-20443, 2011.

[74] S. Koeber, R. Palmer, M. Lauermann, W. Heni, D. L. Elder, D. Korn, M. Woessner, L. Alloatti, S. Koenig, and P. C. Schindler, "Femtojoule electro-optic modulation using a silicon-organic hybrid device," *Light Sci. Appl.(to be published)*, 2014.

[75] D. Korn, R. Palmer, H. Yu, P. C. Schindler, L. Alloatti, M. Baier, R. Schmogrow, W. Bogaerts, S. K. Selvaraja, G. Lepage, M. Pantouvaki, J. Wouters, P. Verheyen, J. V. Campenhout, B. Chen, R. Baets, P. Absil, R. Dinu, C. Koos, W. Freude, and J. Leuthold, "Silicon-organic hybrid (SOH) IQ modulator using the linear electro-optic effect for transmitting 16QAM at 112 Gbit/s," *Optics Express*, vol. 21, pp. 13219-13227, 2013.

[76] D. Patel, S. Ghosh, M. Chagnon, A. Samani, V. Veerasubramanian, M. Osman, and D. V. Plant, "Design, analysis, and transmission system performance of a 41 GHz silicon photonic modulator," *Optics Express*, vol. 23, pp. 14263-14287, 2015.

[77] M. Lauermann, R. Palmer, S. Koeber, P. C. Schindler, D. Korn, T. Wahlbrink, J. Bolten, M. Waldow, D. L. Elder, L. R. Dalton, J. Leuthold, W. Freude, and C. Koos, "Low-power silicon-organic hybrid (SOH) modulators for advanced modulation formats," *Optics Express*, vol. 22, pp. 29927-29936, 2014/12/01 2014.

[78] C. Weimann, P. Schindler, R. Palmer, S. Wolf, D. Bekele, D. Korn, J. Pfeifle, S. Koeber, R. Schmogrow, L. Alloatti, D. Elder, H. Yu, W. Bogaerts, L. R. Dalton, W. Freude, J. Leuthold, and C. Koos, "Silicon-organic hybrid (SOH) frequency comb sources for terabit/s data transmission," *Optics Express*, vol. 22, pp. 3629-3637, 2014.

[79] V. Katopodis, C. Kouloumentas, A. Konczykowska, F. Jorge, P. Groumas, Z. Zhang, A. Beretta, A. Dede, J.-Y. Dupuy, and V. Nodjiadjim, "Serial 100 Gb/s connectivity based on polymer photonics and InP-DHBT electronics," *Optics Express*, vol. 20, pp. 28538-28543, 2012.

[80] V. Katopodis, P. Groumas, Z. Zhang, J.-Y. Dupuy, E. Miller, A. Beretta, L. Gounaridis, J. H. Choi, D. Pech, and F. Jorge, "-Gb/s NRZ-OOK Integrated Transmitter for Intradata Center Connectivity," *Photonics Technology Letters, IEEE*, vol. 26, pp. 2078-2081, 2014.

[81] F. Devaux, Y. Sorel, and J. Kerdiles, "Simple measurement of fiber dispersion and of chirp parameter of intensity modulated light emitter," *Journal of Lightwave Technology*, vol. 11, pp. 1937-1940, 1993.

[82] S. Takahashi, B. Bhola, A. Yick, W. Steier, J. Luo, A. Y. Jen, D. Jin, and R. Dinu, "Photo-Stability Measurement of Electro-Optic Polymer Waveguides With High Intensity at 1550-nm Wavelength," *Journal of Lightwave Technology*, vol. 27, pp. 1045-1050, 2009/04/15 2009.

[83] S. Huang, J. Luo, Z. Jin, X.-H. Zhou, Z. Shi, and A. K.-Y. Jen, "Enhanced temporal stability of a highly efficient guest–host electro-optic polymer through a barrier layer assisted poling process," *Journal of Materials Chemistry*, vol. 22, pp. 20353-20357, 2012.

[84] Z. Shi, J. Luo, S. Huang, B. M. Polishak, X.-H. Zhou, S. Liff, T. R. Younkin, B. A. Block, and A. K.-Y. Jen, "Achieving excellent electro-optic activity and thermal stability in poled polymers through an expeditious crosslinking process," *Journal of Materials Chemistry*, vol. 22, pp. 951-959, 2012.

Xingyu Zhang (S'13–M'13) received the B.S. degree in electrical engineering from Beijing Institute of Technology, Beijing, China, in 2009, the M.S. degree in electrical engineering from University of Michigan, Ann Arbor, MI, USA, in 2010, and the Ph.D degree in electrical engineering from University of Texas, Austin, TX, USA, in 2015. His research focuses on the design, fabrication, and characterization of silicon-polymer hybrid integrated microwave photonic devices for optical interconnects, electro-optic modulation, and electromagnetic wave detection. He has published about 50 peer-reviewed papers in journals and conferences during the Ph.D degree, about 35 of which he first authored, including 3 invited papers and 3 invited talks. Dr. Zhang is the recipient of 2015 SPIE Photonics West Best Student Paper Award, 2014 SPIE Optics and Photonics Best Student Paper Award, 2014 OSA Incubic Milton Chang Student Travel Grant, 2014 SPIE Student Travel Grant, 2015 Chinese Government Award for Outstanding Self-financed Students Abroad, etc. He has so far served as a reviewer for up to 150 papers in 21 journals in his research area, and he received the 2015 OSA Outstanding Reviewer Award for the recognition of his outstanding review work. He is a student member of IEEE, SPIE and OSA. After obtaining his Ph.D, he joined HP Labs as a postdoctoral researcher, with the main research topic of silicon photonics and the long-term goal of achieving a low-power high-speed photonic interconnect system for HP data center business.

Chi-jui Chung received his B.S. degree in mechanical engineering from National Chiao Tung University, Hsinchu, Taiwan, in 2009 and the M.S. degree in power mechanical engineering from National Tsing Hua University, Hsinchu, Taiwan, in 2011. From 2011 to 2014, he was with the Electronics and Opto-Electronics Research Laboratories, Industrial Technology Research Institute, Hsinchu, Taiwan. He is currently working toward the Ph.D. degree at the University of Texas at Austin, TX, USA. His current research interests include the silicon-polymer hybrid integrated microwave photonic devices, including sub-volt photonic crystal waveguide modulators and broadband electromagnetic field sensors.

Amir Hosseini (S'05–M'13), received his B.Sc. degree in Electrical Engineering in 2005 from Sharif University of Technology, Tehran, Iran, M.Sc. degree in Electrical and Computer Engineering in 2007 from Rice University, Houston, TX, and the Ph.D. degree in Electrical and Computer Engineering from the University of Texas at Austin, Texas in 2011.
He has been engaged in research on modeling, design, fabrication and characterization of optical phased array technology, true-time delay lines, and high performance optical modulators. He is a Prince of Wales' scholar in 2011 and recipient of the Ben Streetman Award in 2012, and has authored or co-authored over 70 peer reviewed technical papers. He is a member of IEEE, OSA, and SPIE. He has been serving as the principal investigator for an AFRL sponsored project on polymer optical modulators since 2012.

Harish Subbaraman (M'09), received his M.S. and Ph.D. degrees in Electrical Engineering from the University of Texas at Austin, Texas in 2006 and 2009, respectively. With a strong background in RF photonics and X-band Phased Array Antennas, Dr. Subbaraman has been working on optical true-time-delay feed networks for phased array antennas for the past 8 years. Throughout these years, he has laid a solid foundation in both theory and

experimental skills. His current research areas include printing and silicon nanomembrane based flexible electronic and photonic devices, polymer photonics, slow-light photonic crystal waveguides, carbon nanotube and silicon nanoparticle nanofilm based ink-jet printed flexible electronics, and RF photonics; He has served as a PI on 10 SBIR/STTR Phase I/II projects from NASA, Air Force and Navy. Dr. Subbaraman has over 85 publications in refereed journals and conferences.

Jingdong Luo, received Ph. D. degree in Chemistry from Wuhan University in 2000. He is the senior research scientist at the Department of Materials Science and Engineering, University of Washington. He is the co-founder of Soluxra, LLC, aims at producing cutting-edge high performance functional materials and their hybrid systems to fulfill the diverse customer needs for applications in telecommunication, optical computing, sensing, and clean energy technologies. He led the recent development of a series of high performance EO polymers (such as SEO100, SEO125, SEO250 and SEO500) as new generation high performance (r_{33} values up to 250 pm/V) photonic polymer products. He has dedicated more than ten years of research experience in the field of organic photonics and electronics. He has co-authored more than 160 research papers and texts with numerous scientific citations (> 7,000 times), and holds 13 patents on organic functional materials for opto-electronics and photonics. His major scientific achievements include supramolecular engineering of organic nonlinear optical materials for low driven voltage modulators, efficient pyroelectric poling of organic/polymeric dielectric materials, high performance electro-optic polymers for CPU CMOS and silicon photonic platforms, and aggregation induced emission mechanism for OLED and sensing applications.

Alex K.-Y Jen, is the Boeing-Johnson Chair Professor at the Materials Science and Engineering Department of University of Washington. His research focuses on utilizing molecular, polymeric and biomacromolecular self-assembly to create ordered arrangement of organic, inorganic and hybrid functional materials for photonics, opto-electronics, nanomedicine, and nanotechnology. He has co-authored over 500 papers, given over 350 invited presentations. His work has been widely cited for more than 18,000 times and with a H-index of 71. He is also a co-inventor for more than 50 patents and invention disclosures.

For his pioneering contributions in organic photonics and electronics, he has been elected as Fellow by Materials Research Society (MRS), American Chemical Society (ACS), American Association of the Advancement of Science (AAAS), Optical Society of America (OSA), International Society of Optical Engineering (SPIE), and by Polymeric Materials Science & Engineering (PMSE) Division of ACS. He has also been elected as a Member of Washington State Academy of Sciences in 2011.

He has published about 40 peer-reviewed papers as the first author in journals and conferences during the PhD degree, including some invited papers and invited talks. Mr. Zhang is the recipient of SPIE Optics and Phtonics Best Student Paper Award, OSA Incubic Milton Chang Student Travel Grant, SPIE Student Travel Grant, Engineering Scholarship Award at UT-Austin, Professional Development Award at UT-Austin, and Full Fellowship at UM-Ann Arbor. He has so far served as a reviewer for 19 journals in his research area. He is a student member IEEE, SPIE and OSA.

Robert L. Nelson received the B.S. degree in physics from the University of Wisconsin, Eau Claire, WI, USA, in 1988, and the Ph.D. degree in optics from the University of Rochester, Rochester, NY, USA, in 1999. From 1988 to 1992, he was at Naval Nuclear Power School as an instructor, and since 1999, he is working at the Air Force Research Laboratory, Materials and Manufacturing Directorate, Dayton, OH, USA, as a Research Scientist. His past and current research interests include composite optical materials, photonic crystals, optical and RF metamaterials, and RF photonics materials devices and systems

Charles Y-C. Lee is AFOSR's program manager of the Polymer Chemistry Task in the Directorate of Chemistry and Life Sciences. He received his PhD in Chemistry from University of Wisconsin, Madison, WI, in 1976. He joined the Polymer Branch of the Air Force Materials Laboratory (ML) in 1979. He became a Research Group Leader in 1981. Between 1985 and 1989, he was the Research Leader in the Structural Materials Branch. In 1989 to 1991, he was a Research Group Leader in the Polymer Branch. In 1991, he transferred to AFOSR and became the Program Manager of the Polymer Chemistry Task in Chemistry and Atmospheric Sciences Directorate. He represented AFOSR between 1992 to 1996 to the Air Force Laboratory Demonstration Program (LDP), which was later renamed Laboratory Quality Improvement Program (LQIP). He was selected as an Air Force Research Laboratory Fellow in 1999. He is also the Fellow of American Association for the Advancement of Science, the Fellow of the International Society for Optics and Photonics, the Fellow of Optical Society of America, and the Fellow of the Society of Advanced Material and Process Engineering.

Ray T. Chen (M'91–SM'98–F'04), holds the Keys and Joan Curry/Cullen Trust Endowed Chair at The University of Texas Austin. Chen is the director of the Nanophotonics and Optical Interconnects Research Lab, at the Microelectronics Research Center.

He is also the director of the newly formed AFOSR MURI-Center for Silicon Nanomembrane involving faculty from Stanford, UIUC, Rutgers, and UT Austin. He received his BS degree in Physics in 1980 from the National Tsing Hua University in Taiwan, his MS degree in physics in 1983, and his PhD degree in Electrical Engineering in 1988, both from the University of California. He joined UT Austin in 1992 to start the optical interconnect research program. From 1988 to 1992 Chen worked as a research scientist, manager, and director of the Department of Electro-Optic Engineering at the Physical Optics Corporation in Torrance, California.

Chen served as the CTO, Founder, and Chairman of the Board of Radiant Research, Inc. from 2000 to 2001, where he raised 18 million dollars A-Round funding to commercialize polymer-based photonic devices involving over twenty patents, which were acquired by Finisar in 2002, a publicly traded company in the Silicon Valley (NASDAQ:FNSR). He also serves as the founder and Chairman of the Board of Omega Optics Inc. since its initiation in 2001. Omega Optics has received over five million dollars in research funding.

His research work has been awarded over 120 research grants and contracts from such sponsors as Army, Navy, Air Force, DARPA, MDA, NSA, NSF, DOE, EPA, NIH, NASA, the State of Texas, and private industry. The research topics are focused on three main subjects: (1) Nano-photonic passive and active devices for sensing and interconnect applications, (2) Thin film guided-wave optical interconnection and packaging for 2D and 3D laser beam routing and steering, and (3) True time delay (TTD) wide band phased array antenna (PAA). Experiences garnered through these programs in polymeric and semi-conducting material processing and device integration are pivotal elements for his research work.

Chen's group at UT Austin has reported its research findings in more than 780 published papers, including over 85 invited papers. He holds 30 issued patents. He has chaired or been a program-committee member for more than 110 domestic and international conferences organized by IEEE, SPIE (The International Society of Optical Engineering), OSA, and PSC. He has served as an editor, co-editor or coauthor for over twenty books. Chen has also served as a consultant for various federal agencies and private companies and delivered numerous invited talks to professional societies. Chen is a Fellow of IEEE, OSA, and SPIE. He was the recipient of the 1987 UC Regent's Dissertation Fellowship and the 1999 UT Engineering Foundation Faculty Award, for his contributions in research, teaching and services. He was also the recipient of the 2008 IEEE Teaching Award, and the 2010 IEEE HKN Loudest Professor Award. 2013 NASA Certified Technical Achievement Award for contribution on moon surveillance conformable phased array antenna. During his undergraduate years at the National Tsing Hua University he led the 1979 university debate team to the Championship of the Taiwan College-Cup Debate Contest.

Chen has supervised and graduated 46 PhD students from his research group at UT Austin.